Optically bound colloidal lattices in evanescent optical fields

XIANG HAN[1,2], HUI LUO[1], GUANGZONG XIAO[1,3], AND PHILIP H. JONES[2,*]

[1]College of Opto-Electric Science and Engineering, National University of Defense Technology, Changsha, China, 410073
[2]Department of Physics and Astronomy, University College London, Gower Street, London WC1E 6BT, United Kingdom
[3]State Key Laboratory of Transient Optics and Photonics, Chinese Academy of Sciences, Xi'an, China, 710119
[*]Corresponding author: philip.jones@ucl.ac.uk

Compiled October 7, 2016

In this paper we demonstrate the formation of a stable two-dimensional lattice of colloidal particles in the interference pattern formed by four evanescent optical fields at a dielectric interface. The microspheres are observed to form a two-dimensional square lattice with lattice vectors inclined relative to the beam propagation directions. We use digital video microscopy and particle tracking to measure the Brownian motion of particles bound in the lattice, and use this to characterize fluctuations in the local ordering of particles using the bond orientational order parameter, the probability distribution of which is shown to be a chi-squared distribution. An explanation for the form of this distribution is presented in terms of fluctuations of the modes of a ring of particles connected by springs.

OCIS codes: *(140.7010) Laser trapping; (170.4520) Optical confinement and manipulation; (350.4855) Optical tweezers or optical manipulation.*

http://dx.doi.org/10.1364/ol.XX.XXXXXX

Optical binding [1–3] refers to the spontaneous arrangement of microscopic particles in an intense optical field as a result of multiple scattering between the particles. Although the ability of light to exert a significant force on matter has been widely exploited in the case of manipulating single particles in optical tweezers [4, 5], the phenomenon of optical binding has been much less studied. Optical binding is frequently realized using a pair of counter-propagating Gaussian laser beams, e.g. the output from single-mode optical fibers [6, 7]. In this situation, one-dimensional chains of longitudinally optically bound microscopic particles form where the beams overlap [8]. An alternative means of introducing the intense fields required for optical binding is to use evanescent fields created either at the surface of a prism by a beam incident at the critical angle [9], or around an optical fiber tapered to a sub-micron waist [10]. Transfer of momentum from the evanescent field to microscopic particles immersed in the field results in propulsion of the particles along the direction of beam propagation [9, 11], and the introduction of a counter-propagating field to balance the radiation pressure can produce a stable trap and the formation of stable structures [12–14].

Although microscopic spheres are commonly employed in optical binding, recently the range of particles used has been extended to include gold [15] and silver [16] nanoparticles, and carbon nanotube bundles [17] in differing experimental geometries. The effect of particle size (and shape) is of interest since it was shown that even in a one-dimensional beam geometry a rich variety of two-dimensional particle structures that are strongly dependent on particle size and laser polarization can be formed [18, 19].

In this work we study optical binding of microscopic spheres in a two-dimensional geometry, using an evanescent field formed by two pairs of counter-propagating laser beams. We observe the formation of a stable colloidal lattice with a square symmetry, and characterize fluctuations on the local order of the lattice using the frequency distribution of the local bond orientational order parameter [20]. We present a model that describes the observed frequency distribution by considering the Brownian fluctuations of a ring of four particles surrounding the lattice site at which the order parameter is evaluated. Such an optically bound lattice may be useful for testing models of two-dimensional crystal melting [21, 22].

The experimental apparatus is adapted from our previous work on one-dimensional optical binding [23], and is shown in Fig. 1(a). The beam from a Nd:YAG laser, wavelength $\lambda = 1064$ nm and maximum output power $P_{\max} = 2$ W, is expanded by a telescope and divided into two equal intensity beams by a 50/50 beam splitter. Both beams are focused by lenses (focal lengths $F_1 = F_3 = 150$ mm) onto the planar surface of a near-hemispherical prism, where they intersect at right angles and form waists measuring approximately 70 μm $\times$ 50 μm. The beams are subsequently recollimated (by lenses of focal lengths $F_2 = F_4 = 150$ mm), retro-reflected, and re-focused by the same lenses, such that all four beam waists overlap on the prism surface. Half-wave plates in each beam are used to set the polarization of each beam to be perpendicular to the prism surface. The

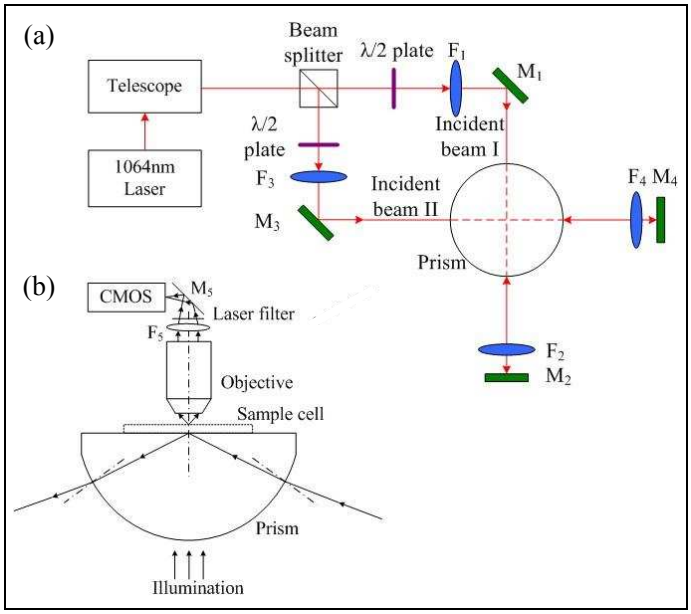

Fig. 1. Experimental apparatus. (a) The laser beam is expanded by a telescope, then split at the 50/50 beam splitter. The lenses F_1 and F_3 focus the two beams which are then collimated and re-focused after retro-reflection by lenses F_2 and F_4 respectively. In this way all four beams are incident on the prism surface at the critical angle for the glass-water interface where they overlap. The two half wave plates ($\lambda/2$ plate) are used to set the polarizations to be perpendicular to the prism surface.

experiment is visualized by illumination using a white LED array, and imaged via a NA = 1.25 oil immersion objective and $F_5 = 175$ mm focal length tube lens onto a 1.3 megapixel CMOS camera. A colored glass filter is used to eliminate scattered laser light as shown in Fig. 1(b).

Samples are made by diluting 0.5 μl of 1 μm diameter silica microspheres solution (initial concentration 50 mg/ml) with 50 μl of deionised water containing 10% of the surfactant Triton-X to prevent the microspheres from irreversibly sticking together or to the plane surface. A cell is made on the lens surface using an adhesive SecureSeal spacer (diameter 9 mm, depth 0.12 mm), filled with diluted bead solution and sealed with a No. 1.5 cover slip.

When only a single pair of counter-propagating beams is used, then for incident laser powers of a few hundred milliwatts the microspheres are observed to spontaneously form optically bound chains parallel to the directions of propagation of the laser beams. When both laser beams are incident on the sample, large numbers of particles accumulate in the intersection region and are observed to form a regular square lattice structure as shown in Fig. 2(a). As is readily seen in Fig. 2(a) the axes of the lattice do not coincide with the xy axes defined by the directions of propagation of the laser beams. In fact, in all our experiments the lattice axes are rotated with respect to the lab xy frame by an angle $\Theta \simeq \pm 22.5^\circ$. Both positive and negative rotations of the lattice are observed to occur with almost equal frequency, and this rotation is reproduced each time the lattice re-forms, e.g. after obstructing the laser beams. It is perhaps not surprising that the colloidal lattice is not congruent with the underlying interference pattern. The difference between the

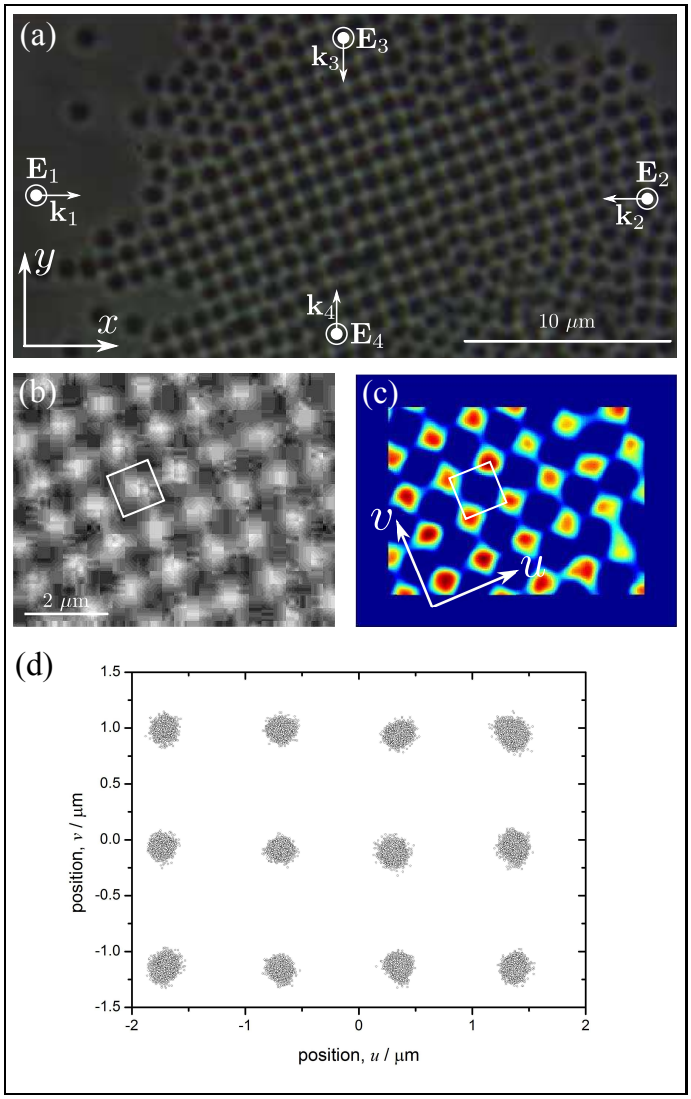

Fig. 2. (a) An optically bound lattice containing over 200 1 μm diameter silica microspheres which forms spontaneously in the counter-propagating evanescent fields. The wavevectors $\underline{k}_i$ $(i = 1 \ldots 4)$ and electric field polarizations $\underline{E}_i$ $(i = 1 \ldots 4)$ are oriented as shown (the scale bar is 10 μm); (b) A reduced area of interest measuring approximately 7.5 μm $\times$ 5.9 μm is used for achieving higher frame rate digital video recording (the scale bar is 2 μm); (c) Image of video frame after spatial filtering and convolution with a Gaussian kernel. The lattice axes u and v are in the directions shown. In parts (b) and (c) a unit cell of the square lattice of side $a = 1.06$ μm is marked; (d) A scatter plot of measured particle positions over 5×10^3 frames in a section of the lattice with axes rotated to lie along the lattice u, v axes.

lattice of our experiments and earlier work demonstrating colloidal lattices such as [2] or [24] is that the lattice is formed in the plane containing the incident and forward-scattered directions. Even for the case of a pair of dipolar particles multiple scattering between them dominates the background field effects to control the dimer position and orientation [25]. Calculations on clusters of cylinders in a three-beam interference pattern [26] show that they are bound in a lattice that has the same symmetry as, but is incommensurate with, the background intensity

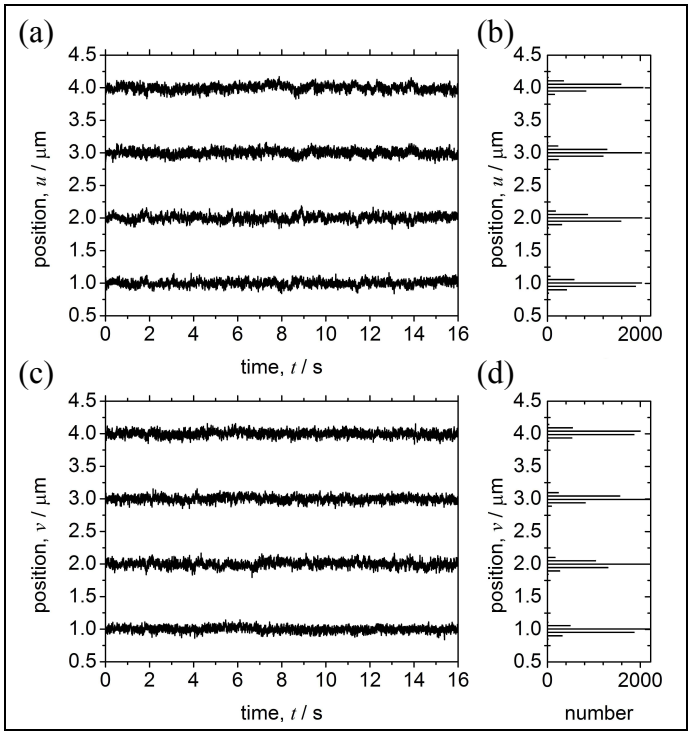

Fig. 3. (a) Brownian position fluctuations of four particles that make up a unit cell of the optically bound lattice in the lattice u-direction; (b) histogram of position fluctuations in the u-direction; (c) Brownian fluctuations of the same four particles in the lattice $v-$direction; (d) histogram of position fluctuations in the v-direction. In all cases the particle positions have been separated by 1 μm for clarity.

due to multiple scattering effects.

We use digital video microscopy and particle tracking [27] to record the Brownian position fluctuations of the particles. A reduced area of interest (measuring approximately 7.5 μm $\times$ 5.9 μm) is used to permit high frame rate digital video recording, as shown in Fig. 2(b). Up to 2×10^4 video frames are recorded with a video frame rate of 307 frames per second. The frames are spatially filtered and subject to convolution by Gaussian kernel. The maxima of the resulting intensity peaks, shown in Fig. 2(c), corresponding to the centroids of the particles can then be tracked with sub-pixel accuracy.

The Brownian fluctuations of the optically bound particles reveal information about the structure of the lattice and strength of the optical binding interaction. From the average particle positions (after subtraction of the center of mass motion of all tracked particles) we determine the lattice constant to be $a = 1.06 \pm 0.01$ μm.

Fig. 3(a) shows the position fluctuations in the $u-$direction for the particles that make up the unit cell of the lattice as marked in figure 2(c). For clarity the average particle positions have been separated by 1 μm. Fig. 3(b) shows the histograms of these fluctuations which are Gaussian distributed. Similarly, Fig. 3(c) shown the position fluctuations of these particles in the lattice $v-$direction, and Fig. 3(d) the Gaussian-distributed histogram of these fluctuations. The Gaussian distribution of position fluctuations suggests that each particle is bound in an (approximately) harmonic potential well that results from the light scattered onto it from all other particles in the lattice. We examine a region shown in Fig. 2(b) which is close to the middle of the lattice to avoid edge effects. From the distribution of fluctuations of the particles in this area we deduce that the curvature of the lattice potential (lattice spring constant) for each particle in this regions is $\langle \kappa_u \rangle = 2.2 \pm 0.1$ pNμm^{-1} in the $u-$direction, and $\langle \kappa_v \rangle = 2.1 \pm 0.1$ pNμm^{-1} in the $v-$direction. The dynamics of particles in the lattice are determined by both optical and hydrodynamic interactions [28] which in this case are difficult to separate since we are not able to image the entire lattice during video microscopy to determine the hydrodynamic coupling.

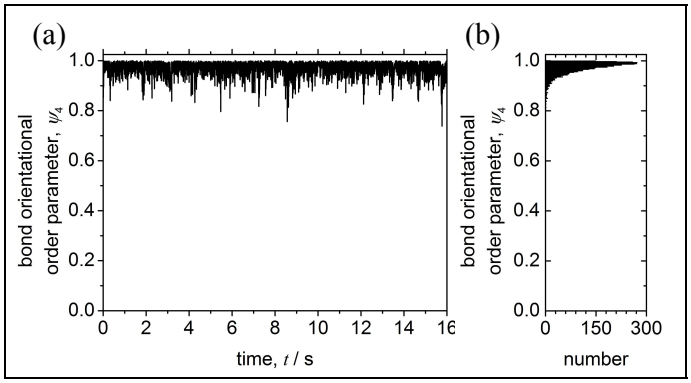

Fig. 4. The bond orientational order parameter, ψ_4 (a) fluctuations of $\psi_4(t)$ measured as a function of time; (b) histogram of fluctuations in ψ_4.

The optically bound colloidal lattice is robust and persists for long times, maintaining the square symmetry. In order to quantify this persistence and order we evaluate the bond orientational order parameter, defined for a particle j in the square lattice as

$$\psi_4 = |\frac{1}{z_j} \sum_{m=1}^{z_j} \exp(4i\theta_m^j)|, \qquad \textbf{(1)}$$

where z_j is the co-ordination number (i.e. the number of nearest neighbors, $z_j = 4$ in this case), and θ_m^j is the angle between the direction of the bond from particle j to particle m and the $x-$axis. For perfect square symmetry, $\psi_4 = 1$. The experimentally determined temporal fluctuations of $\psi_4(t)$ measured at an exemplar particle in the square lattice are shown in Fig. 4(a), with a histogram of fluctuations shown in Fig. 4(b).

To model the distribution of fluctuations in ψ_4 (i.e. p_{Ψ_4}) we re-write the equation for ψ_4 assuming that the amplitude of fluctuations in θ_m^j away from their average positions are small, i.e. $\phi_m = \theta_m^j - \langle \theta_m^j \rangle \ll 1$. In this limit

$$\psi_4 = 1 - \frac{1}{2} \sum_{m \neq m'} (\phi_m - \phi_{m'})^2 = 1 - 2 \sum_{n=1\ldots3} \alpha_n^2, \qquad \textbf{(2)}$$

where α_n ($n = 1 \ldots 3$) are the (higher) modes of a ring of four particles connected by springs [29], represented graphically in Fig. 5(a). Note that the fundamental mode α_0 does not appear in the summation since this mode does not contribute to local distortions of the square. The temporal fluctuations of α_n are shown in figure Fig. 5(b), and histograms of these fluctuations, shown in Fig. 5(c), show that these are normally distributed. Since α_n are normally-distributed random variables, each of the quantities α_n^2 are χ_1^2-distributed. The quantity

$$\Psi_4 = \frac{1 - \psi_4}{2} = \sum_{n=1\ldots3} \alpha_n^2 \qquad \textbf{(3)}$$

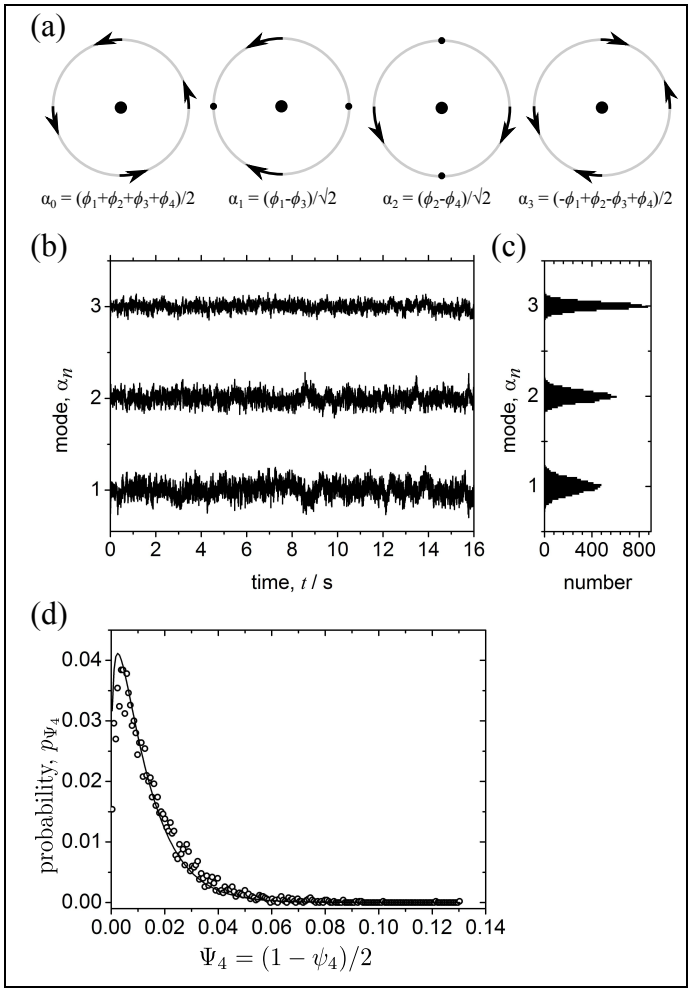

Fig. 5. Mode analysis of thermal fluctuations in the bond orientational order parameter. (a) Illustration of the modes of a four-particle ring, α_n, $n = 0 \ldots 3$; (b) measured fluctuations in the higher modes α_n, $n = 1 \ldots 3$; (c) histogram of mode fluctuations; (d) probability function, p_Ψ (open circles), with prediction based on chi-squared model with effective degrees of freedom $\nu_E = 2.4778$ (line).

is therefore the sum of three chi-squared distributions and is itself chi-squared distributed. Since the variances σ_n are unequal we apply the Satterthwaite approximation to find the effective number of degrees of freedom of the combined distribution as $\nu_E = 2.4778$

The probability distribution p_{Ψ_4} is shown in figure 5(d), where the open circles are the experimental data and the solid line is the modeled distribution based on the measured variances of the modes $\alpha_{n=1,2,3}$, which demonstrates very good agreement. It can be observed that the most probable value of Ψ_4 is not zero, i.e. the most probable instantaneous local ordering of particles is not a square lattice, although the structure on average retains four-fold rotational symmetry.

We have presented here a two-dimensional optically bound colloidal lattice that forms in the interference pattern of two pairs of counter-propagating beams. Analysis of the Brownian motion of the particles in the lattice reveals information about the lattice constant, strength of binding of the particle to the lattice site, and fluctuations in the local ordering. We anticipate that such an optically bound lattice could be useful for testing, e.g., theories of two-dimensional crystal melting.

FUNDING INFORMATION

This work is supported by the Leverhulme Trust. Xiang Han thanks the China Scholarship Council for a visiting studentship.

REFERENCES

1. M. M. Burns, J.-M. Fournier, and J. A. Golovchenko, Phys. Rev. Lett. **63**, 1233–1236 (1989).
2. M. M. Burns, J.-M. Fournier, and J. A. Golovchenko, Science **249**, 749–754 (1990).
3. K. Dholakia and P. Zemánek, Rev. Mod. Phys. **82**, 1767 (2010).
4. A. Ashkin, J. M. Dziedzic, J. E. Bjorkholm, and S. Chu, Opt. Lett. **11**, 288–290 (1986).
5. P. H. Jones, O. M. Maragò, and G. Volpe, *Optical Tweezers: Principles & Applications* (Cambridge University Press, Cambridge, 2015), 1st ed.
6. S. A. Tatarkova, A. E. Carruthers, and K. Dholakia, Phys. Rev. Lett. **89**, 283901 (2002).
7. W. Singer, M. Frick, S. Bernet, and M. Ritsch-Marte, J. Opt. Soc. Am. B **20**, 1568–1574 (2003).
8. R. Gordon, M. Kawano, J. T. Blakely, and D. Sinton, Phys. Rev. B **77**, 245125 (2008).
9. S. Kawata and T. Sugiura, Opt. Lett. **17**, 772–774 (1992).
10. G. Brambilla, G. S. Murugan, J. S. Wilkinson, and D. J. Richardson, Opt. Lett. **32**, 3041–3043 (2007).
11. S. E. Skelton, M. Sergides, R. Patel, E. Karczewska, O. M. Maragò, and P. H. Jones, J. Quant. Spectrosc. Radiat. Transfer **113**, 2512–2520 (2012).
12. V. Garcés-Chávez, K. Dholakia, and G. C. Spalding, Appl. Phys. Lett. **86**, 031106 (2005).
13. P. J. Reece, E. M. Wright, and K. Dholakia, Phys. Rev. Lett. **98**, 203902 (2007).
14. M. C. Frawley, I. Gusachenko, V. G. Truong, M. Sergides, and S. Nic Chormaic, Opt. Express **22**, 16322–16334 (2014).
15. V. Demergis and E.-L. Florin, Nano Lett. **12**, 5756–5760 (2012).
16. Z. Yan, R. A. Shah, G. Chado, S. K. Gray, M. Pelton, and N. F. Scherer, ACS Nano **7**, 1790–1802 (2013).
17. O. M. Maragò, P. H. Jones, P. G. Gucciardi, G. Volpe, and A. C. Ferrari, Nat. Nanotechnology **8**, 807–819 (2013).
18. C. D. Mellor and C. D. Bain, ChemPhysChem **7**, 329–332 (2006).
19. J. M. Taylor, L. Y. Wong, C. D. Bain, and G. D. Love, Opt. Express **16**, 6921–6929 (2008).
20. P. J. Steinhardt, D. R. Nelson, and M. Ronchetti, Phys. Rev. B **28**, 784–805 (1983).
21. J. M. Kosterlitz and D. J. Thouless, Journal of Physics C: Solid State Physics **6**, 1181 (1973).
22. K. Zahn, R. Lenke, and G. Maret, Phys. Rev. Lett. **82**, 2721–2724 (1999).
23. X. Han and P. H. Jones, Opt. Lett. **40**, 4042–4045 (2015).
24. J. Baumgartl, J. Dietrich, J. Dobnikar, C. Bechinger, and H. H. von Grunberg, Soft Matter **4**, 2199–2206 (2008).
25. J. Luis-Hita, J. J. Sáenz, and M. I. Marqués, ACS Photonics **3**, 1286–1293 (2016).
26. T. M. Grzegorczyk, B. A. Kemp, and J. A. Kong, J. Opt. Soc. Am. A **23**, 2324–2330 (2006).
27. J. C. Crocker and D. G. Grier, J. Colloid Interface Sci. **179**, 298–310 (1996).
28. M. Šiler, T. Čižmár, and P. Zemánek, Applied Physics Letters **100**, 051103 (2012).
29. R. Di Leonardo, S. Keen, J. Leach, C. D. Saunter, G. D. Love, G. Ruocco, and M. J. Padgett, Phys. Rev. E **76**, 061402 (2007).

INFORMATIONAL FIFTH PAGE

REFERENCES

1. M. M. Burns, J.-M. Fournier, and J. A. Golovchenko, "Optical binding," Phys. Rev. Lett. **63**, 1233–1236 (1989).
2. M. M. Burns, J.-M. Fournier, and J. A. Golovchenko, "Optical matter: crystallization and binding in intense optical fields," Science **249**, 749–754 (1990).
3. K. Dholakia and P. Zemánek, "Colloquium: gripped by light: optical binding," Rev. Mod. Phys. **82**, 1767 (2010).
4. A. Ashkin, J. M. Dziedzic, J. E. Bjorkholm, and S. Chu, "Observation of a single-beam gradient force optical trap for dielectric particles," Opt. Lett. **11**, 288–290 (1986).
5. P. H. Jones, O. M. Maragò, and G. Volpe, *Optical Tweezers: Principles & Applications* (Cambridge University Press, Cambridge, 2015), 1st ed.
6. S. A. Tatarkova, A. E. Carruthers, and K. Dholakia, "One-dimensional optically bound arrays of microscopic particles," Phys. Rev. Lett. **89**, 283901 (2002).
7. W. Singer, M. Frick, S. Bernet, and M. Ritsch-Marte, "Self-organized array of regularly spaced microbeads in a fiber-optical trap," J. Opt. Soc. Am. B **20**, 1568–1574 (2003).
8. R. Gordon, M. Kawano, J. T. Blakely, and D. Sinton, "Optohydrodynamic theory of particles in a dual-beam optical trap," Phys. Rev. B **77**, 245125 (2008).
9. S. Kawata and T. Sugiura, "Movement of micrometer-sized particles in the evanescent field of a laser beam," Opt. Lett. **17**, 772–774 (1992).
10. G. Brambilla, G. S. Murugan, J. S. Wilkinson, and D. J. Richardson, "Optical manipulation of microspheres along a subwavelength optical wire," Opt. Lett. **32**, 3041–3043 (2007).
11. S. E. Skelton, M. Sergides, R. Patel, E. Karczewska, O. M. Maragò, and P. H. Jones, "Evanescent wave optical trapping and transport of micro-and nanoparticles on tapered optical fibers," J. Quant. Spectrosc. Radiat. Transfer **113**, 2512–2520 (2012).
12. V. Garcés-Chávez, K. Dholakia, and G. C. Spalding, "Extended-area optically induced organization of microparticles on a surface," Appl. Phys. Lett. **86**, 031106 (2005).
13. P. J. Reece, E. M. Wright, and K. Dholakia, "Experimental observation of modulation instability and optical spatial soliton arrays in soft condensed matter," Phys. Rev. Lett. **98**, 203902 (2007).
14. M. C. Frawley, I. Gusachenko, V. G. Truong, M. Sergides, and S. Nic Chormaic, "Selective particle trapping and optical binding in the evanescent field of an optical nanofiber," Opt. Express **22**, 16322–16334 (2014).
15. V. Demergis and E.-L. Florin, "Ultrastrong optical binding of metallic nanoparticles," Nano Lett. **12**, 5756–5760 (2012).
16. Z. Yan, R. A. Shah, G. Chado, S. K. Gray, M. Pelton, and N. F. Scherer, "Guiding spatial arrangements of silver nanoparticles by optical binding interactions in shaped light fields," ACS Nano **7**, 1790–1802 (2013).
17. O. M. Maragò, P. H. Jones, P. G. Gucciardi, G. Volpe, and A. C. Ferrari, "Optical trapping and manipulation of nanostructures," Nat. Nanotechnology **8**, 807–819 (2013).
18. C. D. Mellor and C. D. Bain, "Array formation in evanescent waves," ChemPhysChem **7**, 329–332 (2006).
19. J. M. Taylor, L. Y. Wong, C. D. Bain, and G. D. Love, "Emergent properties in optically bound matter," Opt. Express **16**, 6921–6929 (2008).
20. P. J. Steinhardt, D. R. Nelson, and M. Ronchetti, "Bond-orientational order in liquids and glasses," Phys. Rev. B **28**, 784–805 (1983).
21. J. M. Kosterlitz and D. J. Thouless, "Ordering, metastability and phase transitions in two-dimensional systems," Journal of Physics C: Solid State Physics **6**, 1181 (1973).
22. K. Zahn, R. Lenke, and G. Maret, "Two-stage melting of paramagnetic colloidal crystals in two dimensions," Phys. Rev. Lett. **82**, 2721–2724 (1999).
23. X. Han and P. H. Jones, "Evanescent wave optical binding forces on spherical microparticles," Opt. Lett. **40**, 4042–4045 (2015).
24. J. Baumgartl, J. Dietrich, J. Dobnikar, C. Bechinger, and H. H. von Grunberg, "Phonon dispersion curves of two-dimensional colloidal crystals: the wavelength-dependence of friction," Soft Matter **4**, 2199–2206 (2008).
25. J. Luis-Hita, J. J. Sáenz, and M. I. Marqués, "Arrested dimer's diffusion by self-induced back-action optical forces," ACS Photonics **3**, 1286–1293 (2016).
26. T. M. Grzegorczyk, B. A. Kemp, and J. A. Kong, "Trapping and binding of an arbitrary number of cylindrical particles in an in-plane electromagnetic field," J. Opt. Soc. Am. A **23**, 2324–2330 (2006).
27. J. C. Crocker and D. G. Grier, "Methods of digital video microscopy for colloidal studies," J. Colloid Interface Sci. **179**, 298–310 (1996).
28. M. Šiler, T. Čižmár, and P. Zemánek, "Speed enhancement of multiparticle chain in a traveling standing wave," Applied Physics Letters **100**, 051103 (2012).
29. R. Di Leonardo, S. Keen, J. Leach, C. D. Saunter, G. D. Love, G. Ruocco, and M. J. Padgett, "Eigenmodes of a hydrodynamically coupled micron-size multiple-particle ring," Phys. Rev. E **76**, 061402 (2007).